Applied Catalysis B: Environmental 117–118 (2012) 406–413

Contents lists available at SciVerse ScienceDirect

Applied Catalysis B: Environmental

journal homepage: www.elsevier.com/locate/apcatb

Evaluation of ion exchange-modified Y and ZSM5 zeolites in Cr(VI) biosorption and catalytic oxidation of ethyl acetate

B. Silva[a,*], H. Figueiredo[a], O.S.G.P. Soares[b], M.F.R. Pereira[b], J.L. Figueiredo[b], A.E. Lewandowska[c], M.A. Bañares[c], I.C. Neves[d], T. Tavares[a]

[a] IBB – Institute for Biotechnology and Bioengineering, Centre of Biological Engineering, University of Minho, Campus de Gualtar, 4710-057 Braga, Portugal
[b] Laboratory of Catalysis and Materials (LCM), Associate Laboratory LSRE-LCM, Chemical Engineering Department, Faculty of Engineering, University of Porto, Rua Dr. Roberto Frias, 4200-465 Porto, Portugal
[c] Catalytic Spectroscopy Laboratory, Institute of Catalysis and Petrochemistry, CSIC, E-28049 Madrid, Spain
[d] Department of Chemistry, Centre of Chemistry, University of Minho, Campus de Gualtar, 4710-057 Braga, Portugal

ARTICLE INFO

Article history:
Received 2 December 2011
Received in revised form 30 January 2012
Accepted 1 February 2012
Available online 10 February 2012

Keywords:
Y zeolite
ZSM5 zeolite
Ion exchange
Cr(VI) biosorption
Catalytic oxidation
Ethyl acetate

ABSTRACT

The aim of this work was the evaluation of the performance of two zeolites with different structures (FAU and MFI) and acidity properties in the biosorption of Cr(VI) and catalytic oxidation of ethyl acetate. The starting zeolites, Y (FAU) and ZSM5 (MFI), were modified by ion exchange treatments with $NaNO_3$ in order to obtain zeolites with different acidity and sodium content. A biosorption system consisting of a bacterium, *Arthrobacter viscosus*, supported on the different zeolites was used for Cr(VI) reduction and removal from solution. The best removal efficiencies and uptake of chromium, above 90% and 14 $mg_{Cr}/g_{zeolite}$ respectively, were achieved for Y zeolites due to their higher ion exchange capacity in comparison with ZSM5 zeolites. The ion exchange treatment did not produce considerable changes on the uptake process performed by the modified zeolites. Y and ZSM5 zeolites were characterized by ICP-AES, SEM, NH_3 chemisorption, XRD and N_2 adsorption. Y and ZSM5 zeolites obtained after biosorption presented chromium loadings between 0.92 and 1.20%, and were successfully reused as catalysts in the oxidation of ethyl acetate. The chromium-loaded ZSM5 zeolites were considerably more active and selective towards CO_2 than chromium-loaded Y zeolites, essentially due to their different framework structure, textural and acidity properties. The different sodium content of Y and ZSM5 zeolites did not produce marked changes in the catalytic behaviour of these catalysts.

1. Introduction

Zeolites are widely used in several applications such as ion exchange, adsorption, heterogeneous catalysis, biosorption supports, polymer catalytic degradation and also attract interest in materials science for the development of functional materials and in nanotechnology [1–7].

Zeolites are crystalline aluminosilicates with structures consisting of three dimensional frameworks of SiO_4 and AlO_4 tetrahedra linked through oxygen bridges. These structures possess a net negative charge that is the result of the isomorphous replacement of Si^{4+} by Al^{3+} in the crystal lattice [1,8]. This negative charge is balanced by cations (Na^+, K^+ or Ca^{2+}) that are exchangeable with other cations in solution such as heavy metal ions. Thus, zeolites have great selectivity for cation exchange, but little or no affinity for anions, such as Cr(VI) species ($Cr_2O_7^{2-}$, $HCrO_4^-$, CrO_4^{2-}) [1,9,10]. As hexavalent chromium is a very toxic and xenobiotic pollutant, the research of cost-effective technologies for its removal is an important issue. Due to the inability of zeolites to remove anions, some authors studied the performance of surfactant-modified zeolites for the removal of Cr(VI). However, low uptakes were achieved after the modification of the zeolites surface. Noroozifar et al. [11] investigated the capacity of a natural zeolite modified by HMNA-Br_2 to remove Cr(VI) and obtained a maximum uptake of 2.60 $mg_{Cr(VI)}/g_{zeolite}$. As well, Yusof et al. [12] studied the adsorption of Cr(VI) by HDTMA-modified NaY zeolite and achieved uptake values no higher than 1.66 $mg_{Cr(VI)}/g_{zeolite}$.

In this work, a biosorption system consisting of a bacteria supported on a zeolite is used for hexavalent chromium removal. The ability of *Arthrobacter viscosus* for Cr(VI) reduction and removal was demonstrated in previous studies [9,13]. The bacteria perform the reduction of Cr(VI) anions to cationic Cr(III) species that can be easily exchanged by the zeolite. This step of reduction allows the entrapment of the metal in the zeolite, otherwise steric limitations and charge repulsions would not permit the zeolite loading with the chromium anionic species. An advantage of using this system

* Corresponding author.
E-mail address: bsilva@deb.uminho.pt (B. Silva).

0926-3373/$ – see front matter © 2012 Elsevier B.V. All rights reserved.
doi:10.1016/j.apcatb.2012.02.002

for the treatment of wastewater contaminated with metals is the reutilization of the obtained metal-loaded zeolites as catalysts for oxidation reactions of organic compounds. After the biosorption process, the zeolite loaded with Cr can be used as a competitive and selective catalyst to be applied in catalytic oxidation of volatile organic compounds [14,15]. Thus, this process presents a double benefit as chromium can be recovered from contaminated water and be reused in catalytic reactions.

The catalytic properties of zeolites are essentially related to their shape selectivity, pore structure, acidity and thermal stability. Although zeolites are well known to have optimum catalytic performances in petroleum refining, recently these materials have gained interest as supports or catalysts for the combustion of volatile organic compounds (VOC). Recent works demonstrated the applicability and efficiency of FAU [16–18] and MFI zeolites [17,19–21] as catalysts for VOC oxidation. Both zeolites used in this work have three dimensional structures. The framework of Y zeolite (FAU-type structure) is based on sodalite cages that are joined by oxygen bridges between the hexagonal faces. Eight sodalite cages are linked together, forming a large central cavity or supercage with a diameter of 11.8 Å. The supercages share a 12-membered ring with an open diameter of 7.4 Å [22–24]. This wide aperture gives access to the microporosity and to the active sites for a wide range of VOC [16]. ZSM5 zeolite (MFI-type structure) is a high silica zeolite that is composed of several *pentasil* units linked together by oxygen bridges to form *pentasil* chains. The *pentasil* chains are interconnected by oxygen bridges to form corrugated sheets with 10-ring holes. ZSM5 is a medium pore zeolite with pore diameters of 5.4–5.6 Å that are defined by these 10 member oxygen rings [22–25]. Because the pore openings are 10-rings rather than 12-rings, the shape selectivity for sorption and catalysis is distinctly different from that of FAU-type zeolite [24].

Apart from the geometrical aspects related to the pore structure, the composition of zeolites may be modified by several treatments that confer different properties to these materials, depending on their specific application. One of the main properties of zeolites is associated to their acidity and the most common method used to modify acidity is the ion exchange treatment [8,18]. The aim of this work is to evaluate the effect of the zeolite structure and modification of their acidity, obtained by ion exchange treatments, in Cr(VI) biosorption and in their further catalytic reutilization in the oxidation of ethyl acetate. This VOC was selected as model compound for the evaluation of the catalytic behaviour of modified Y and ZSM5 zeolites loaded with chromium, since in previous studies [15] this was the only compound for which total oxidation was achieved over Cr-Y catalysts.

2. Experimental

2.1. Materials and reagents

A. viscosus was obtained from the Spanish Type Culture Collection of the University of Valencia. Aqueous potassium dichromate solutions were prepared by diluting $K_2Cr_2O_7$ (Panreac) in distilled water. HY (CBV 400) and ZSM5 (CBV 3024E) zeolites were obtained from Zeolyst International in powder form and were calcined at 500 °C during 8 h under a dry air stream prior to use. The zeolite ZSM5 was available in the ammonium form. After heating, ammonium is transformed into NH_3 and H^+. NH_3 desorbs and the presence of protons increases the number of acid sites. The protonic form of ZSM5 (HZSM5) was obtained after that calcination. The zeolite Y was available in the protonic form (HY). Aqueous sodium nitrate solutions used for ion exchange treatment were prepared by diluting $NaNO_3$ (Riedel-de Haën) in distilled water.

All glassware used for experimental purposes was washed in 10% nitric acid to remove any possible interference by other metals.

2.2. Methods

2.2.1. Ion exchange treatments

HY and HZSM5 zeolites were used as the starting materials and were modified by ion exchange treatments with $NaNO_3$. The modified zeolites were prepared by two ion exchange treatments [8], designated as A and B. The first treatment (A) consisted of exchanging 20 g of each zeolite (HY and HZSM5) with 500 mL of a 1 M $NaNO_3$ solution in a 1000 mL Erlenmeyer flask with a stirrer, at room temperature, during 24 h. After this treatment, the modified zeolite samples were designated as $H(Na)_AY$ and $H(Na)_AZSM5$. In the second treatment (B), the same procedure was performed three times with a 1.5 M $NaNO_3$ solution, the obtained samples being identified as $H(Na)_BY$ and $H(Na)_BZSM5$. The modified zeolites were separated by centrifugation, washed with deionized water, dried in an oven at 60 °C for 8 h and calcined at 500 °C during 8 h under a dry air stream.

2.2.2. Preparation of the biomass

A medium with 10 g/L of glucose, 5 g/L of peptone, 3 g/L of malt extract and 3 g/L of yeast extract was used for the microorganism growth. The medium was sterilized at 121 °C for 20 min, cooled to room temperature, inoculated with bacteria and kept at 28 °C for 24 h with moderate stirring in an incubator. The cells were then harvested by centrifugation at 7000 rpm for 15 min and re-suspended in a pre-established volume of residual culture medium (obtained after the microorganism growth) in order to obtain a concentrated suspension and provide the desired biomass concentration to be used in the biosorption assays.

2.2.3. Biosorption assays

Batch experiments were conducted in 250 mL Erlenmeyer flasks using 15 mL of the *A. viscosus* suspension previously prepared, with a biomass concentration of 5 g/L, 150 mL of a potassium dichromate solution, with an initial concentration of 100 mg_{Cr}/L, and 1.0 g of each zeolite. The solution pH was regularly maintained at pH 4, using H_2SO_4 or NaOH solutions. The Erlenmeyer flasks were kept at 28 °C, with moderate stirring. Samples of 1 mL were taken, centrifuged and analyzed for chromium quantification.

After the biosorption studies, the Cr-loaded zeolites were centrifuged, dried in a oven at 60 °C and finally calcined at 500 °C during 8 h under a dry air stream, in order to remove the organic matter from bacteria. The samples were designated as Cr-HY, Cr-$H(Na)_AY$, Cr-$H(Na)_BY$, Cr-HZSM5, Cr-$H(Na)_AZSM5$ and Cr-$H(Na)_BZSM5$.

2.2.4. Analysis of chromium ions in solution

Hexavalent chromium that remained in solution was quantified by measuring absorbance at 540 nm of the purple complex of Cr(VI) with 1,5-diphenylcarbazide, in acidic solution [26]. For total chromium quantification, the Cr(III) present in solution was first oxidized to Cr(VI) at high temperature by the addition of potassium permanganate previous to the reaction with 1,5-diphenylcarbazide.

2.2.5. Characterization procedures

The zeolite samples were characterized by X-ray diffraction (XRD), scanning electron microscopy (SEM), N_2 adsorption isotherms, elemental chemical analyses (ICP-AES) and NH_3 chemisorption.

Powder X-ray diffraction patterns were recorded using a Philips Analytical X-ray model PW1710 BASED diffractometer system. Scans were taken at room temperature, using Cu Kα radiation in a 2θ range between 5° and 65° at a scan rate of 2°/min.

Table 1
Sodium content and total acidity of the starting and modified zeolites.

Sample	$Na_{initial}$ (%)[a]	Total acidity (cm^3 NH_3/g)[b]
HY	1.80	25.5
$H(Na)_AY$	1.95	20.1
$H(Na)_BY$	2.50	19.4
HZSM5	0.08	23.3
$H(Na)_AZSM5$	0.79	18.4
$H(Na)_BZSM5$	1.10	17.9

[a] Determined by chemical analysis (ICP-AES).
[b] Determined by NH_3 chemisorption.

The morphology of the zeolite samples was evaluated by Scanning Electron Microscopy (SEM), using a Leica Cambridge S360. Previously, the solid samples were coated with Au in vacuum to avoid surface charging using a Fisons Instruments SC502 sputter coater.

The textural characterization of the zeolites was based on the N_2 adsorption isotherms (−196 °C) using an automatic Micromeritics ASAP-2000 apparatus. The samples were previously outgassed at 140 °C for 2 h. Surface areas were calculated by the BET equation, taking a value of 0.162 nm^2 for the cross section of the adsorbed N_2 molecule at −196 °C. The micropore volume (V_{micro}) and external surface area (S_{ext}) were calculated by the *t*-method. The total pore volume (V_p), i.e., the sum of micropore and mesopore volumes, was estimated from the nitrogen uptake at a relative pressure of about 0.99. The mesopore volume (V_{meso}) was obtained by subtracting the micropore volume from the total pore volume.

Elemental chemical analyses were performed by Inductively Coupled Plasma Atomic Emission Spectrometry (ICP-AES), using a Philips ICP PU 7000 Spectrometer, after acid digestion of the samples.

The ammonia chemisorption experiments were performed on an ASAP-2000 apparatus, according to Rojas et al. [27]. The samples (200 mg) were pre-treated at 250 °C for 0.5 h and then cooled to 100 °C under He flow, in order to remove water from the zeolite [28]. The pre-treated samples were exposed to 5% NH_3/He, with subsequent flushing with helium at 100 °C for 1 h to remove the physisorbed ammonia. The acidity values were determined from the difference between ammonia adsorption and desorption isotherms.

2.2.6. Catalytic experiments

The catalytic tests were performed using similar conditions as reported by Bastos et al. [29]. After the biosorption experiments, the zeolite samples Cr-HY, Cr-$H(Na)_BY$, Cr-HZSM5 and Cr-$H(Na)_BZSM5$ were used as catalysts in the oxidation of ethyl acetate. Each catalyst sample (50 mg), previously calcined, was diluted with an inert (carborundum) having the same size as the catalyst particles (0.2–0.5 mm), in order to minimize temperature gradients. Prior to the reaction, the catalyst was pretreated in air flow at 400 °C for 1 h, and then cooled to room temperature. The catalytic oxidation of ethyl acetate was performed under atmospheric pressure in a fixed-bed reactor, consisting of a U-shaped quartz tube of 6 mm internal diameter, placed inside a temperature controlled electrical furnace. Temperature in the reaction zone was measured by a K type thermocouple placed in the middle of the catalyst bed. The flow rate of the reacting stream was 150 cm^3/min (measured at room temperature and pressure), which corresponds to a space velocity of 16,000 h^{-1} (determined in terms of total bed volume), with an ethyl acetate concentration of 4000 mg_{carbon}/m^3 (1000 ppm). The temperature was increased at 2.5 °C/min between room temperature and 500 °C. The gas mixture at the reactor outlet was analyzed by a CO_2 non-dispersive infrared (NDIR) sensor Vaisala GMT220 and a total volatile organic compounds analyzer MiniRAE2000. The reaction was carried out in two cycles of increasing and decreasing temperature. The conversion into CO_2 (X_{CO_2}) was calculated as $X_{CO_2} = F_{CO_2}/(v \cdot F_{VOC,in})$, where $F_{VOC,in}$ is the inlet molar flow rate of VOC ($C_{VOC,in}$ is the corresponding concentration), F_{CO_2} is the outlet molar flow rate of CO_2 and v is the number of carbon atoms in the VOC molecule (for ethyl acetate, $v = 4$).

3. Results

3.1. Modified Y and ZSM5 zeolites

Y and ZSM5 zeolites were submitted to ion-exchange treatments in order to obtain different acidic properties, as acidity plays an important role in the overall process. Sodium content and total acidity were measured and results are presented in Table 1.

The results of chemical analyses reveal that the initial sodium content of HY zeolite is significantly higher than that of HZSM5 zeolite. This is explained by the difference between the Si/Al ratios of the zeolites framework [30]. HY and HZSM5 zeolites have Si/Al ratios of 2.80 and 15.0, respectively. As HY zeolite has a lower Si/Al ratio, the aluminium content in the framework is higher. Therefore, the concentration of charge-balancing cations is higher in HY zeolite, in this case H^+ and Na^+, because each cation compensates the negative charge arising from an Al atom in the framework.

As expected, the content of sodium increased for both Y and ZSM5 zeolites after the ion exchange treatments (A and B). The zeolites $H(Na)_AY$ and $H(Na)_BY$, obtained after each ion exchange, presented an increase of sodium content of about 8% and 39%, respectively, in comparison to the starting zeolite HY. In the case of HZSM5, the increase of sodium concentration after the treatments was even more significant. After the ion exchange treatments A and B, the zeolites $H(Na)_AZSM5$ and $H(Na)_BZSM5$ presented a sodium content that was almost 10 times and 14 times higher, respectively, than the starting HZSM5 zeolite.

With regard to acidity, the values presented in Table 1 represent the total acidity, i.e., the total amount of acid sites of the zeolites that correspond to the quantity of chemisorbed NH_3. As it can be observed, the acidity of the starting HY and HZSM5 zeolites decreased after the ion exchange treatments. The acidity of zeolites is related with Brønsted and Lewis acid sites, both contributing to the total acidity of the solid [31,32]. The Brønsted sites are acidic hydroxyl groups bridging silicon to framework aluminium in the zeolite structure, while the Lewis sites are associated with extra-framework aluminium oxide species [31,33]. It was demonstrated that the ion exchange treatments of zeolites with $NaNO_3$ solutions led to the decrease of the concentration of Brønsted acid sites due to the substitution of the proton in bridging hydroxyl groups by Na^+ [31,34]. The results obtained in this work are in agreement with those studies. For both HY and HZSM5 zeolites the total acidity decreased about 21% after the ion exchange treatment A, and about 23% after the treatment B. This means that even after the most severe ion exchange treatment (B), the acidity of the zeolites did not decrease considerably in comparison with the smoother ion exchange treatment (A). Therefore, the decrease in the acidity values was not proportional to the increase observed in sodium content.

In order to study the morphology of Y and ZSM5 zeolites, the solid samples were characterized by scanning electron microscopy (SEM) before and after the ion exchange treatment. The SEM micrographs are shown in Fig. 1.

Analysing the micrographs presented in Fig. 1, it can be observed that FAU and MFI zeolites have different morphology and particle size. The starting HY zeolite presents well formed cubic particles with average size of about 0.6–0.8 μm. Similar morphology and particle size were observed for the modified zeolite $H(Na)_BY$, obtained

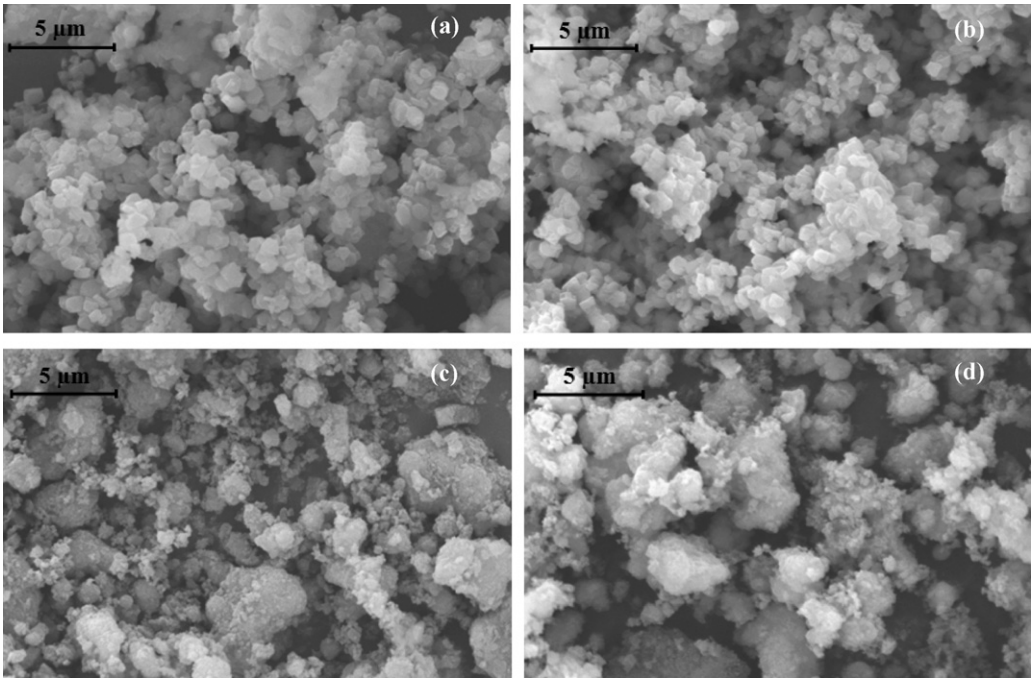

Fig. 1. SEM photographs of the starting and modified zeolites: HY (a), $H(Na)_BY$ (b), HZSM5 (c) and $H(Na)_BZSM5$ (d).

after the most severe ion exchange treatment. For ZSM5 zeolites, it can be seen that the individual particles form larger and irregular aggregates, being therefore difficult to determine the mean size of the primary particles from the SEM image. Comparing the photographs of the starting and the modified zeolites, HZSM5 and $H(Na)_BZSM5$ respectively, no significant differences on morphology and particle size were found. Therefore, it can be concluded that the morphology of Y and ZSM5 zeolites remained practically unchanged after the ion exchange treatments performed.

3.2. Biosorption of Cr(VI)

The modified Y and ZSM5 zeolites were studied as supports for the biosorption of Cr(VI), using *A. viscosus*. The experiments were conducted at pH 4, since it was demonstrated in a previous work [35] that this is the most favourable pH for the reduction and removal of chromium by the combined system bacteria/zeolite. In this section, the role of the structure and acidic properties of the zeolite on the removal performance of Cr(VI) from solution was investigated. Fig. 2 shows the time-dependent concentration of Cr(VI) and total Cr for the different zeolites in study. The total Cr concentration represents the sum of Cr(VI) and Cr(III) concentration values.

Analyzing the concentration profiles presented in Fig. 2, a significant decrease of Cr(VI) and total Cr concentration in the first 7 days of contact time can be observed for all the zeolites tested. As the solution was maintained at pH 4, the high concentration of protons in solution promoted the reduction of Cr(VI) to Cr(III) performed by the bacterium. After the formation of Cr(III) through a reduction process, it is exchanged by the zeolite and removed from solution, and therefore the total Cr concentration decreases, as it was observed for all the zeolites. It is important to refer that the bacterium by itself is able to retain chromium ions through electrostatic binding to functional groups of the biomass surface, as it was thoroughly discussed in a previous work [35]. Therefore, the depletion of total Cr results from the combined contribution of the bacterium and the zeolite. The main goal of this work is to investigate the contribution of the different zeolites tested on the removal of chromium.

No significant differences were observed in the concentration profiles of Cr(VI) in the experiments with the starting and the modified Y zeolites. However, an improvement on the removal of total Cr can be observed with the modified zeolites $H(Na)_AY$ and $H(Na)_BY$, in comparison to the starting HY zeolite. This improvement was more evident as the contact time increased. The higher removal of total Cr observed in the assays with the modified Y zeolites reveals that these zeolites were able to exchange a larger amount of trivalent chromium and therefore had a higher selectivity towards Cr(III) than that of HY zeolite.

With ZSM5 zeolites it was not observed the same trend as for Y zeolites. In the first 7 days of contact time, a better removal rate of Cr(VI) and total Cr was observed for the modified zeolites $H(Na)_AZSM5$ and $H(Na)_BZSM5$. However, at the end of the contact period the lowest total Cr concentration was attained with the starting HZSM5 zeolite.

The removal efficiencies and uptake of total Cr for the different zeolites in study are presented in Fig. 3. The uptake is expressed as the amount of chromium removed from solution per initial mass of zeolite.

It can be observed that ZSM5 zeolites presented removal efficiencies about 30% lower than those achieved by Y zeolites at the end of the contact time. As discussed above, ZSM5 zeolites have higher Si/Al ratio than Y zeolites, and therefore a lower number of framework aluminium atoms and a lower amount of compensating cations. As a result, the ion exchange capacity of ZSM5 zeolites is lower than that of HY zeolites, as shown by the lower removal efficiencies of total Cr.

After the ion exchange treatment, the modified zeolites $H(Na)_AZSM5$ and $H(Na)_BZSM5$ presented lower removal efficiencies and uptake of total Cr in comparison with the starting zeolite. However, the differences were not considerable which allows concluding that the ion exchange treatments did not affect significantly the removal performance of these zeolites. In opposition, for the biosorption experiments with the modified zeolites $H(Na)_AY$ and $H(Na)_BY$, an improvement of total Cr removal and uptake of about 16% after the ion exchange treatments was observed, in comparison with the starting HY zeolite. Among the different zeolites tested, the best removal efficiency and uptake value, 96% and

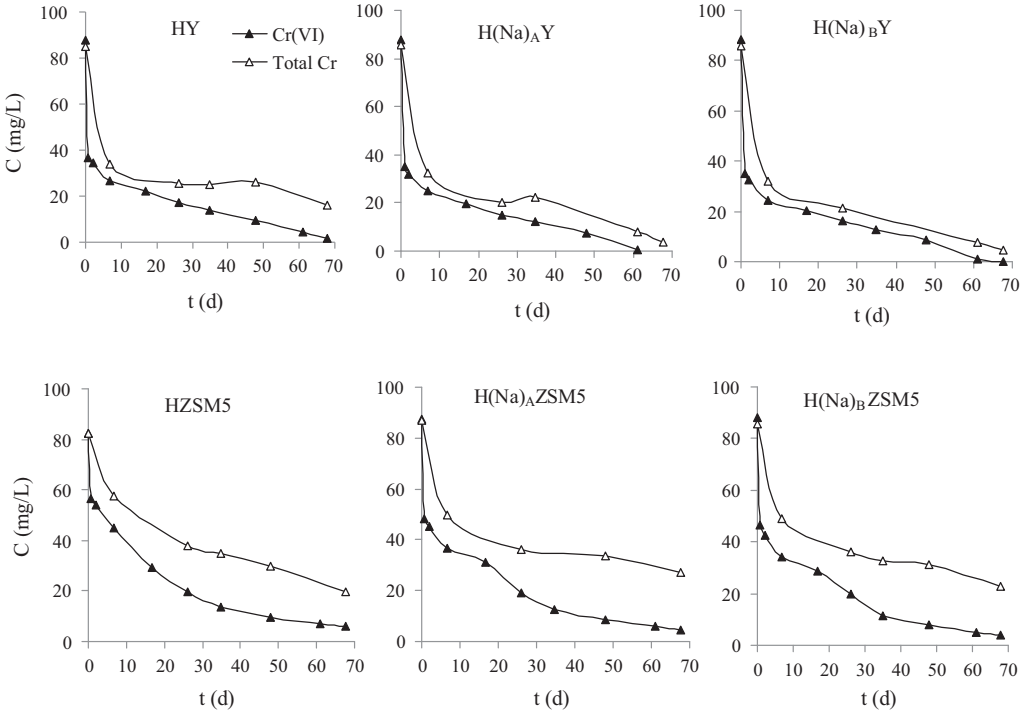

Fig. 2. Concentration of Cr(VI) and total Cr as a function of contact time, during the biosorption assays with *A. viscosus* supported on the different zeolites. Experiments conducted at pH 4, with an initial Cr(VI) concentration of 100 mg/L and biomass concentration of 5 g/L.

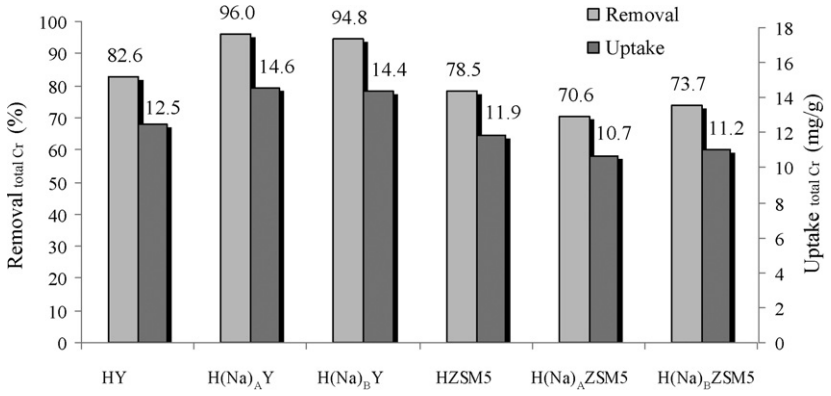

Fig. 3. Removal efficiencies and uptake of total Cr for the biosorption assays performed with *A. viscosus* supported on Y and ZSM5 zeolites. Experiments at pH 4, initial Cr(VI) concentration of 100 mg/L and biomass concentration of 5 g/L.

14.6 $mg_{Cr}/g_{zeolite}$, respectively, were achieved for the biosorption assay with $H(Na)_AY$.

After the biosorption experiments, the chromium-loaded zeolites were analysed for sodium and chromium quantification, and the results are presented in Table 2. As expected and in accordance with the above discussion, the content of chromium in ZSM5 zeolites was lower than that of Y zeolites, due to their lower ion exchange capacity. Although some differences were observed in the removal of total Cr with the modified Y and ZSM5 zeolites, the final chromium content of the zeolites did not change considerably after the ion exchange treatments. Comparing the initial and final sodium content of the zeolites (see also Table 1) a significant decrease of sodium can be observed after the biosorption, which is an indication of the good ion exchange performance of the zeolites.

Table 2
Sodium and chromium content of the zeolites after biosorption.

Sample	Na_{final} (%)[a]	Cr (%)[a]
Cr-HY	0.22	1.10
Cr-$H(Na)_AY$	0.24	1.10
Cr-$H(Na)_BY$	0.44	1.20
Cr-HZSM5	0.07	0.93
Cr-$H(Na)_AZSM5$	0.11	0.95
Cr-$H(Na)_BZSM5$	0.18	0.92

[a] Determined by chemical analyses (ICP-AES).

3.3. Characterization procedures

The structures of Y and ZSM5 zeolites, before and after ion exchange treatment and biosorption, were characterized by X-ray diffraction. The XRD patterns obtained for the different zeolites are illustrated in Fig. 4.

The XRD patterns obtained for Y and ZSM5 zeolites are in agreement with the characteristic diffraction patterns of these zeolites, in terms of peak positions and their relative intensities. The XRD spectra of the starting zeolites, HY and HZSM5, showed a well

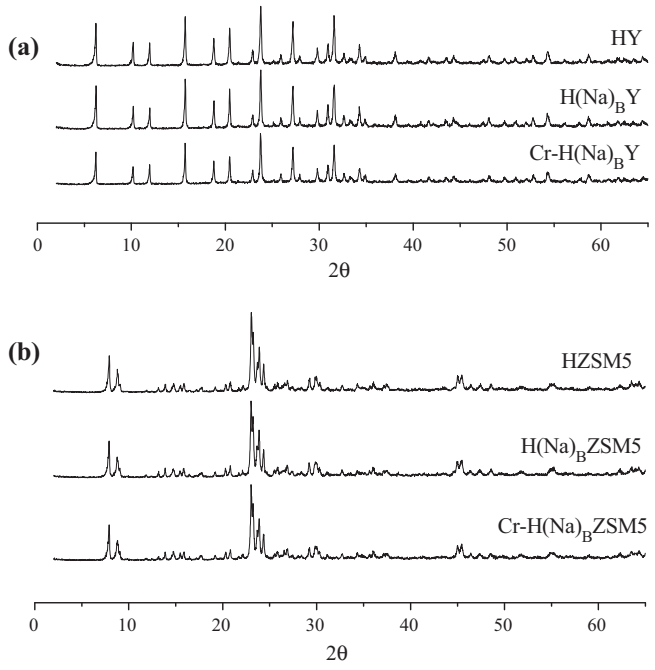

Fig. 4. XRD patterns of zeolites Y (a) and ZSM5 (b) before and after the ion exchange treatment and biosorption of Cr(VI).

crystallized framework and a low background that is an indication of the absence of amorphous phase in these zeolites. For both modified zeolites, obtained after the ion exchange treatment B, $H(Na)_BY$ and $H(Na)_BZSM5$, the XRD patterns are very similar to that of the respective starting zeolite. However, after the biosorption of Cr(VI) some loss of intensity of the peaks can be observed in the XRD patterns of Cr-$H(Na)_BY$ and Cr-$H(Na)_BZSM5$ zeolites. This reveals a decrease in crystallinity of the chromium-loaded zeolites in comparison with the zeolites before biosorption. No diffraction peaks assigned to chromium species occur for Cr-$H(Na)_BY$ and Cr-$H(Na)_BZSM5$ zeolites. Such absence suggests a high dispersion of chromium through the zeolites.

Furthermore, the XRD patterns were used to calculate the average crystal size and the relative crystallinity of the different zeolites. The average crystal sizes were estimated using the Scherrer equation (Eq. (1)). In the case of the zeolite Y, the average size was estimated from the reflection peak [5 5 5] position of the *hkl* indices. For the zeolite ZSM5 it was used the most intense peak.

$$D = \frac{K\lambda}{B\cos\theta} \quad (1)$$

where D is the crystal size, K is a constant (0.9), λ the X-ray wavelength ($\lambda = 0.1542$ nm), B the peak width at a half-height (in radians) and θ the Bragg's angle of diffraction (in radians).

The relative crystallinity of the modified zeolites was calculated by comparing the average intensities of the most intense peaks with that of the parent zeolite, HY or HZSM5, assuming 100% of crystallinity for the starting material. The calculations were made according to the standard methods ASTM D 3906 and ASTM D 5758, for Y and ZSM5 zeolites, respectively. Table 3 summarizes the crystal size and relative crystallinity of the starting and modified Y and ZSM5 zeolites.

It may be observed that the modified zeolites $H(Na)_BY$ and $H(Na)_BZSM5$ maintained about 90% of crystallinity after the ion exchange treatment B, as compared to the respective starting HY and HZSM5. Thus, even the most severe ion exchange treatment used in this work (treatment B) did not modify significantly the zeolites structures. After the biosorption of Cr(VI), a slight loss of crystallinity is also observed, due to the introduction of chromium into Y and ZSM5 zeolites. Finally, the average crystal size of Y and ZSM5 zeolites were of the same order of magnitude, ranging from 44 to 50 nm, which is an additional evidence of the conservation of the zeolite structure after the ion exchange treatment and biosorption of Cr(VI).

Table 3
Structural properties of Y and ZSM5 zeolites determined from XRD.

Sample	Crystal size (nm)	Relative crystallinity (%)
HY	48	100
$H(Na)_BY$	44	93
Cr-$H(Na)_BY$	47	85
HZSM5	40	100
$H(Na)_BZSM5$	50	90
Cr-$H(Na)_BZSM5$	50	75

The textural characterization of Y and ZSM5 zeolites obtained from nitrogen adsorption isotherms is presented in Table 4. As it may be observed, ZSM5 zeolites presented lower surface areas and micropore volumes and higher external surface areas in comparison with Y zeolites. These textural properties are intrinsically related to the different structures and pore geometry of the zeolites. No significant changes in the textural properties of the zeolites were observed after the ion exchange treatment B. However, for the zeolite Cr-$H(Na)_BY$ after the biosorption process a decrease of about 16% of the surface area and pore volume was observed. On the other hand, the decrease of the surface area of Cr-$H(Na)_BZSM5$ zeolite was less pronounced (about 4.5%), although an increase of the mesopore volume and a decrease of the microporosity were observed.

3.4. Catalytic experiments

The catalytic performance of Y and ZSM5 zeolites obtained after biosorption of Cr(VI) was evaluated in the oxidation of ethyl acetate. The light-off curves of a standard experiment consisted in two cycles of increasing temperature, keeping the temperature constant for 1 h and decreasing it. The performance of all catalysts was always compared using the decreasing temperature step.

The comparison of the catalytic performance of the different chromium-loaded zeolites in the oxidation of ethyl acetate at a concentration of 4000 mg_C/m^3 is shown in Fig. 5. Table 5 summarizes the temperatures corresponding to complete conversion of ethyl acetate ($T_{100\%}$) and to the maximum conversion into CO_2 ($X_{CO_2\,max}$), for the different catalysts tested.

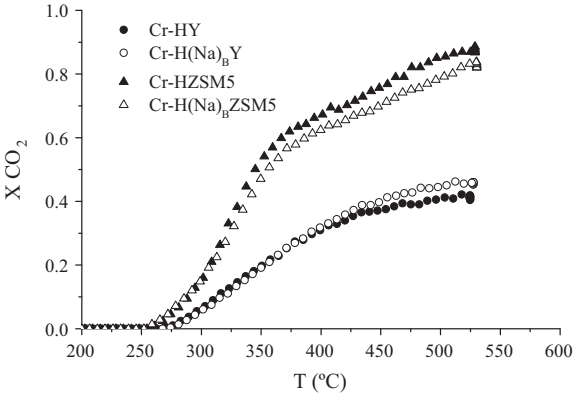

Fig. 5. Light-off curves for the oxidation of ethyl acetate on Cr-HY, Cr-$H(Na)_BY$, Cr-HZSM5 and Cr-$H(Na)_BZSM5$ for the cooling step, at a VOC concentration of 4000 mg_C/m^3.

Table 4
Textural characterization of Y and ZSM5 zeolites by N_2 adsorption.

Sample	S_{BET} (m^2/g)[a]	S_{ext} (m^2/g)[b]	V_p (cm^3/g)[c]	V_{micro} (cm^3/g)[b]	V_{meso} (cm^3/g)[d]
HY	611	51	0.318	0.257	0.061
$H(Na)_BY$	625	53	0.334	0.262	0.072
Cr-$H(Na)_BY$	524	46	0.282	0.219	0.063
HZSM5	374	97	0.213	0.125	0.088
$H(Na)_BZSM5$	362	76	0.208	0.130	0.078
Cr-$H(Na)_BZSM5$	346	88	0.210	0.117	0.093

[a] Surface area calculated from BET equation.
[b] External surface area and micropore volume calculated by the *t*-method.
[c] Total pore volume determined from the amount adsorbed at $P/P_0 = 0.99$.
[d] Mesopore volume calculated by the difference $V_p - V_{micro}$.

The results reveal that the chromium-loaded ZSM5 zeolites presented a significantly higher activity and selectivity towards CO_2 in comparison with the chromium-loaded Y zeolites. For all catalysts tested, ethyl acetate conversion (data not shown) started at 210 °C, and CO_2 began to be produced at 260 °C for ZSM5 catalysts and at 280 °C for Y catalysts. For chromium-loaded ZSM5 zeolites, the complete conversion of ethyl acetate was achieved at temperatures almost 100 °C lower than those required for chromium-loaded Y zeolites (Table 5).

The maximum yield of CO_2, above 80%, was attained with the Cr-HZSM5 and Cr-$H(Na)_BZSM5$ catalysts, while the conversion into CO_2 was not higher than 45% with the Y catalysts. The differences in activity and selectivity observed between Y and ZSM5 zeolites loaded with chromium are related to the structural, acidic and textural properties of these supports.

The acidity of the support has an influence on the activity of catalysts. ZSM5 zeolites have lower total acidity (Table 1) in comparison with Y zeolites, caused by their lower aluminium content. As a result, ZSM5 zeolites have a lower density of acid sites, and probably this lower acidity makes these catalysts more active for ethyl acetate oxidation comparing with Y zeolites. The negative influence of the acidity on the catalytic activity of zeolites was also reported by Tsou et al. [36]. These authors studied the catalytic oxidation of methyl-isobutyl-ketone (MIBK) over two Pt/zeolite catalysts with different Si/Al ratio and acidity, Pt/HFAU(5) and Pt/HFAU(47). The results showed that the catalyst with higher acidity, Pt/HFAU(5), presented lower conversion into CO_2, in spite of the higher load of platinum.

Moreover, dark spots were observed in chromium-loaded Y zeolites after the catalytic tests, which indicate the deposition of carbonaceous compounds during the reaction. On the contrary, ZSM5 catalysts presented a homogeneous surface and no dark spots were observed. Due to their different framework structure, with a pore opening of 10-rings, which avoid the formation of irreversibly adsorbed compounds, ZSM5 catalysts present a better stability for the oxidation of ethyl acetate. In addition, the formation of carbonaceous compounds was probably enhanced in the case of Y catalysts, due to their higher acidity. Tsou et al. [36] have also reported a higher extent of coke formation over the catalyst with higher acidity, Pt/HFAU(5), during the catalytic oxidation of MIBK.

Table 5
Temperatures corresponding to 100% of ethyl acetate conversion and maximum yield of CO_2, for an initial VOC concentration of 4000 mg_C/m^3.

Catalyst	$T_{100\%}$ (°C)[a]	$X_{CO_2\,max}$ (%)[b]	T (°C)[c]
Cr-HY	483	41	500
Cr-$H(Na)_BY$	440	45	
Cr-HZSM5	371	87	520
Cr-$H(Na)_BZSM5$	375	83	

[a] Temperatures for complete conversion of ethyl acetate.
[b] Calculated from the equation: $X_{CO_2} = F_{CO_2}/(4 \cdot F_{VOC,in})$.
[c] Temperatures for the maximum conversion into CO_2.

Another important characteristic of the catalyst is its mesoporosity, since this property affects the catalytic performance, coke deposition and catalyst deactivation [37,38]. As discussed above, ZSM5 zeolites presented higher mesoporosity and external surface areas compared to Y zeolites (Table 4). It is known that mesopores reduce mass transfer limitations for reactants and products by effectively decreasing the path length for diffusion [39]. Therefore, the diffusion of ethyl acetate and product molecules to and from the reaction sites was probably easier in ZSM5 catalysts in comparison with Y catalysts, due to their framework structure.

Thus, in spite of ZSM5 catalysts having lower chromium content and surface area than Y zeolites, acidic, structural and textural properties played an important role in their activity and selectivity during the oxidation of ethyl acetate.

Concerning the ion exchange treatment B, no marked differences in the behaviour of Y and ZSM5 catalysts were observed, which is an indication that the extension of sodium exchange did not affect substantially the catalytic properties of the zeolites. With ZSM5 catalysts, similar profiles of ethyl acetate conversion (not shown) were observed for Cr-$H(Na)_BZSM5$ and Cr-HZSM5, the latter revealing a slight improvement of selectivity towards CO_2 at temperatures above 330 °C. With Y catalysts, the complete conversion of ethyl acetate performed by Cr-$H(Na)_BY$ was achieved at 440 °C, i.e., at a temperature 43 °C lower than that required for Cr-HY. In terms of selectivity, a very slight improvement of CO_2 yield for the Cr-$H(Na)_BY$ catalyst was observed, only at temperatures above 435 °C.

In our previous work [15], the oxidation of ethyl acetate over Cr-NaY zeolites was studied. The starting zeolite NaY presented a sodium content of 7.76% and a total acidity of 7.53 cm^3 NH_3/g. For an ethyl acetate concentration of 4000 mg_C/m^3, the maximum conversion into CO_2, 57%, was achieved at a temperature of 520 °C. Comparing the results of the previous and the present work, it can be concluded that Y zeolites with higher content of sodium and therefore lower total acidity present slightly better selectivity towards CO_2 in the catalytic oxidation of ethyl acetate. This is a further indication that the oxidation of ethyl acetate is favoured over less acidic supports. So far, no other studies were published regarding the complete oxidation of ethyl acetate over Y zeolites loaded with transition metals. On the other hand, some studies were found in literature reporting the use of metal-loaded ZSM5 zeolites as catalysts for the oxidation of ethyl acetate. A comparison of the catalytic performance of the different ZSM5 catalysts and respective operational conditions used are shown in Table 6. Abdullah et al. [40] studied the catalytic oxidation of ethyl acetate over a high silica ZSM5 zeolite with chromium content of 0.98% and obtained similar results in comparison with this work, in terms of activity and selectivity. For the other studies presented in Table 6, no information was given about the selectivity of the catalysts towards CO_2. However, in terms of ethyl acetate conversion it can be concluded that chromium-loaded ZSM5 catalysts revealed to be the most active, followed by Cu-ZSM5, Ni-ZSM5, Ag-ZSM5 and Mn-ZSM5.

Table 6
Ethyl acetate oxidation over different metal-loaded ZSM5 catalysts.

Catalyst	Cr-HZSM5This work	Cr-ZSM5[40]	Cu-ZSM5[19]	Mn-ZSM5[20]	Ni-ZSM5[20]	Ag-ZSM5[21]
Metal content (%)	0.93	0.98	5	2.38	2.25	1.9
Si/Al	15	240	12	14	14	14
$m_{catalyst}$ (mg)	50	200	200	200	200	200
$C_{ethyl\ actetate}$ (ppm)	1000	2000	–	730	730	1000
GHSV (h^{-1})[a]	16,000	32,000	32,000	–	–	30,000
$X_{ethyl\ actetate}$ (%)	100	100	100	75	97	93
T_1 (°C)[b]	371	350	390	500	500	450
X_{CO_2} (%)	88	80	–	–	–	–
T_2 (°C)[c]	525	500	–	–	–	–

[a] Gas hourly space velocity, defined as volume of gas feed per hour per volume of catalyst bed.
[b] Temperature for maximum ethyl acetate conversion.
[c] Temperature for the maximum conversion into CO_2.

4. Conclusions

A combined biosorption system consisting of a bacterium, *A. viscosus*, supported on Y and ZSM5 zeolites revealed to be efficient on the removal of Cr(VI) from aqueous solution. The ion exchange treatments with $NaNO_3$ performed to the starting HY and HZSM5 zeolites led to the increase of sodium content and consequently to the decrease of total acidity. The modified zeolites obtained after the ion exchange process showed similar performances on chromium removal in comparison with the starting zeolites, which indicates that the incorporation of sodium did not produce considerable changes on the uptake process. During biosorption process, Y zeolites presented higher efficiencies of chromium removal due to their higher ion exchange capacity in comparison with ZSM5 zeolites. After the biosorption of Cr(VI), the different chromium-loaded zeolites were successfully used as catalysts for the complete oxidation of ethyl acetate. ZSM5 catalysts showed higher activity and selectivity towards CO_2 than Y zeolites. No considerable differences were observed in the catalytic behaviour of Y and ZSM5 catalysts with different content of sodium, which reveals that the extension of sodium exchange did not affect substantially the catalytic properties of the zeolites. Other important factors such as structural and textural properties as well as the acidity of the supports played an important role in the activity and selectivity of the catalysts during ethyl acetate oxidation.

Acknowledgments

B. Silva, H. Figueiredo and O.S.G.P. Soares thank FCT-Portugal (Fundação para a Ciência e Tecnologia) for the concession of their PhD grants. A.E. Lewandowska thanks the Spanish Ministry of Science and Innovation for a "Juan de la Cierva" postdoctoral position. This work was partially funded by the Centre of Biological Engineering and Centre of Chemistry (University of Minho, Portugal) through a POCTI project (ref: POCTI-SFA-3-686), by the Spanish Ministry of Science and Innovation (CTQ2008-04261/PPQ) and by FCT and FEDER under Programs POCI 2010 and COMPETE, Project PTDC/AMB/69065/2006.

References

[1] P. Panneerselvam, N. Thinakaran, K.V. Thiruvenkataravi, M. Palanichamy, S. Sivanesan, J. Hazard. Mater. 159 (2008) 427–434.
[2] A. Corma, H. Garcia, Eur. J. Inorg. Chem. (2004) 1143–1164.
[3] H. Figueiredo, B. Silva, C. Quintelas, M.M.M. Raposo, P. Parpot, A.M. Fonseca, A.E. Lewandowska, M.A. Bañares, I.C. Neves, T. Tavares, Appl. Catal. B-Environ. 94 (2010) 1–7.
[4] I. Kuzniarska-Biernacka, K. Biernacki, A.L. Magalhães, A.M. Fonseca, I.C. Neves, J. Catal. 278 (2011) 102–110.
[5] I.C. Neves, G. Botelho, A.V. Machado, P. Rebelo, S. Ramôa, M.F.R. Pereira, A. Ramanathan, P. Pescarmona, Polym. Degrad. Stab. 92 (2007) 1513–1519.
[6] I.C. Neves, C. Cunha, M.R. Pereira, M.F.R. Pereira, A.M. Fonseca, J. Phys. Chem. C 114 (2010) 10719–10724.
[7] R.A. Van Santen, G.J. Kramer, Chem. Rev. 95 (1995) 637–660.
[8] I.C. Neves, G. Botelho, A.V. Machado, P. Rebelo, J. Eur. Polym. 42 (2006) 1541–1547.
[9] B. Silva, H. Figueiredo, C. Quintelas, I.C. Neves, T. Tavares, Micropor. Mesopor. Mater. 116 (2008) 555–560.
[10] Y. Zeng, H. Woo, G. Lee, J. Park, Micropor. Mesopor. Mater. 130 (2010) 83–91.
[11] M. Noroozifar, M. Khorasani-Motlagh, M.N. Gorgij, H.R. Naderpour, J. Hazard. Mater. 155 (2008) 566–571.
[12] A.M. Yusof, N.A.N.N. Malek, J. Hazard. Mater. 162 (2009) 1019–1024.
[13] B. Silva, H. Figueiredo, I.C. Neves, T. Tavares, Proc. World Acad. Sci. Eng. Technol. 33 (2008) 59–62.
[14] H. Figueiredo, I.C. Neves, C. Quintelas, T. Tavares, M. Taralunga, J. Mijoin, P. Magnoux, Appl. Catal. B-Environ. 66 (2006) 274–280.
[15] B. Silva, H. Figueiredo, V.P. Santos, M.F.R. Pereira, J.L. Figueiredo, A.E. Lewandowska, M.A. Bañares, I.C. Neves, T. Tavares, J. Hazard. Mater. 192 (2011) 545–553.
[16] R. Beauchet, J. Mijoin, I. Batonneau-Gener, P. Magnoux, Appl. Catal. B-Environ. 100 (2010) 91–96.
[17] E. Díaz, S. Ordóñez, A. Vega, J. Coca, Micropor. Mesopor. Mater. 83 (2005) 292–300.
[18] J. Tsou, P. Magnoux, M. Guisnet, J.J.M. Órfão, J.L. Figueiredo, Appl. Catal. B-Environ. 51 (2004) 129–133.
[19] S.A. Hosseini, A. Niaei, D. Salari, F. Aghazadeh, Chin. J. Chem. 28 (2010) 143–148.
[20] A. Jodaei, D. Salari, A. Niaei, M. Khatamian, S.A. Hosseini, J. Environ. Sci. Health Part A Toxic/Hazard. Subst. Environ. Eng. 46 (2011) 50–62.
[21] A. Jodaei, D. Salari, A. Niaei, M. Khatamian, N. Çaylak, Environ. Technol. 32 (2011) 395–406.
[22] Database of Zeolite Structures, International Zeolite Association (IZA-SC). www.iza-structure.org/databases/.
[23] C. Baerlocher, L.B. McCusker, D.H. Olson, Atlas of Zeolite Framework Types, sixth ed., Elsevier, Netherlands, 2007.
[24] L.B. McCusker, C. Baerlocher, in: J. Cejka, H.v. Bekkum (Eds.), Studies in Surface Science and Catalysis, Elsevier, 2005, pp. 41–64.
[25] S. Sang, F. Chang, Z. Liu, C. He, Y. He, L. Xu, Catal. Today 93–95 (2004) 729–734.
[26] D. Eaton, L.S. Clesceri, A.E. Greenberg, Standard Methods for the Examination of Water and Wastewater, American Public Health Association (APHA), Washington, 1995.
[27] E. Rojas, M. Calatayud, M.O. Guerrero-Pérez, M.A. Bañares, Catal. Today 158 (2010) 178–185.
[28] M.A. Bañares, G. Mestl, Advances in Catalysis, Academic Press, 2009, pp. 43–128.
[29] S.S.T. Bastos, J.J.M. Órfão, M.M.A. Freitas, M.F.R. Pereira, J.L. Figueiredo, Appl. Catal. B-Environ. 93 (2009) 30–37.
[30] K. Sato, Y. Nishimura, N. Matsubayashi, M. Imamura, H. Shimada, Micropor. Mesopor. Mater. 59 (2003) 133–146.
[31] G.S. Nivarthy, K. Seshan, J.A. Lercher, Micropor. Mesopor. Mater. 22 (1998) 379–388.
[32] J. Weitkamp, Solid State Ionics 131 (2000) 175–188.
[33] K. Wang, X. Wang, G. Li, Catal. Commun. 8 (2007) 324–328.
[34] M. Guisnet, P. Magnoux, Catal. Today 36 (1997) 477–483.
[35] B. Silva, H., Figueiredo, C., Quintelas, I.C., Neves, T. Tavares, Improved biosorption system for Cr(VI) reduction and removal using Y zeolite, unpublished results.
[36] J. Tsou, P. Magnoux, M. Guisnet, J.J.M. Órfão, J.L. Figueiredo, Appl. Catal. B-Environ. 57 (2005) 117–123.
[37] J. Kim, M. Choi, R. Ryoo, J. Catal. 269 (2010) 219–228.
[38] K. Sato, Y. Nishimura, H. Shimada, Catal. Lett. 60 (1999) 83–87.
[39] K.P. Jong, A.J. Koster, A.H. Janssen, U. Ziese, in: J. Cejka, H.v. Bekkum (Eds.), Studies in Surface Science and Catalysis, vol. 157, Elsevier, 2005, pp. 225–242.
[40] A.Z. Abdullah, M.Z.A. Bakar, S. Bhatia, Catal. Commun. 4 (2003) 555–560.